© Universiti Tun Hussein Onn Malaysia Publisher's Office

IJIE

http://penerbit.uthm.edu.my/ojs/index.php/ijie
ISSN : 2229-838X e-ISSN : 2600-7916

The International Journal of Integrated Engineering

Investigating The Surface Characteristics of Dip Coated 3D Printed ABS Specimens

Poornaganti Satyanarayana[1], Yeole Shivraj Narayan[1*], Kode Jaya Prakash[1], Jyotsna Cherukuri[2], Maneiah D.[3]

[1]Department of Mechanical Engineering,
VNR Vignana Jyothi Institute of Engineering and Technology, Hyderabad, 500090, INDIA

[2]Department of Chemistry,
VNR Vignana Jyothi Institute of Engineering and Technology, Hyderabad, 500090, INDIA

[3]Department of Mechanical Engineering,
CMR Technical Campus, Hyderabad, 501401, INDIA

*Corresponding Author

DOI: https://doi.org/10.30880/ijie.2023.15.05.006
Received 10 January 2023; Accepted 25 May 2023; Available online 19 October 2023

Abstract: In the past few years, FDM based polymer 3D printing process has flourished mainly with ABS filaments as a thermoplastic source. Food packing, medical, marine and agriculture industries employ devices and other usable items made of polymers. Utilizing layered fabrication components in these areas compel them to have self-cleansing, anti-freezing and corrosion resistant surfaces. It is generally complex and expensive to prepare hydrophobic coatings. The present work is related to the development of a surface coating on 3D printed ABS specimens with the mentioned properties. 3D printed specimens were fabricated using Flash Forge 3D printer without any modifications, and the hydrophobic coatings were achieved by dip coating process using Tricalcium phosphate-chitin solutions with a ratio of 70:30. Static contact angle measurement was employed in gaging wettability impact on dip coated 3D printed specimens. By using digital vernier calipers and profilometer (SJ410), dimensional accuracy and surface roughness were assessed pre and post-coating. According to ASTM D570-98, water absorption tests were conducted at different time intervals. Results of the experiment showed that the hydrophobic solutions had been successfully synthesized. The maximum contact angle was achieved for solution 1 (4g of tricalcium phosphate solution with 0.3g chitin solution) i.e., 109.3°. Improvement in the texture of 3D printed ABS surfaces was observed after dip coating. Dip-coated 3D printed ABS specimens exhibited minimal absorption based on their weight gain per area.

Keywords: 3D printing, hydrophobic coating, surface roughness, dimensional accuracy, surface wettability absorption

1. Introduction

In additive manufacturing, layer-by-layer material is added to form tailor-made parts through digital fabrication. Prototyping or the final production of a product can be accomplished with the aid of a 3D printer. Many products can be produced using 3D printers, ranging from medical components to leisure articles. For fast prototyping, polymers have been the most commonly used. As mechanical support for medical implants and inert materials, polymers have played an important role in developing biomaterials and medical devices [1]. To produce 3D models and prototypes, FDM is the most popular and cost-effective technique. Plastics such as polycarbonate, polylactic acid, ABS, PEEK, and even nanocomposites can be 3D printed using this technology. Moreover, 3D printers can utilize natural fibers, which are

*Corresponding author: shivarajyeole@vnrvjiet.in

biodegradable and have better properties [2]. In ABS, the three constituents' acrylonitrile (A), butadiene (B), and styrene (S) form a terpolymer. Various resins can be made by changing the ratio of the three monomers. Among its features are the ability to resist corrosion by chemicals and heat, the ability to be molded thermoplastically, and the ability to be electrically conductive. A material like ABS offers a wide range of applications, convenient access to raw materials, and excellent overall quality at a reasonable price [3]. Application of wax and Ni-Co-Cr alloy coating on ABS tend to improve its characteristics [4]. The tribological properties of polymers can be improved by coating them with graphene [5]. PLA surfaces can be synthesized using an alkali-wet chemical for one hour (1h AT) or six hours (6h AT), followed by nHA [6]. An nHA coating was applied to PLA flat discs and 3D-printed scaffolds to produce biocompatible polyvinylpyrrolidone hydrogels [7]. An acetone vapor and hot air chemical finishing procedure are suitable for ABS material, while acetone, a colorless solvent, is used for smooth surfaces [8-9]. Chemicals such as acetone, ester, and chloride solvents can also be used to improve the roughness of specimens [10]. Aimed at assessing surface finish, 3D printed objects were coated using XTC-3D [11]. The amount of material deposited during 3D printing is impacted by the specimen's fillet radius and printer settings, leading to gradual degradation [12]. FDM printed ABS and PLA polymers were optimized using CO2 laser scanning [13]. The surface quality of ABS parts significantly improved by employing cold vapor of dimethyl ketone on it [14,15].

A variety of processes, including laser surface ablation and mechanical machining, have been used to fabricate micro or nanoscale surface structures utilizing hydrophobic materials. Coatings with hydrophobic properties can be deposited electrochemically, chemically etched, photolithographically, sprayed, phase separated, sol-gelled, self-assembled and electrospun. These, however, are time-consuming and expensive [16]. The maximum angle on the GF-2200 hydrophobic coating on nanoceramic resin at ambient temperature is 110° [4]. The ACNTB-SiO_2-KH570 and epoxy (EP) adhesive precursor was used to create a super-hydrophobic composite coating [17]. Hydrophobic coatings consisting of silica nanoparticles and MEK lessened the influence of surface coatings on the mechanical attributes of layered deposition components [18]. The printed specimens were compared using a CAD model to ensure that they were dimensionally correct. Measurements were made at three points using Vernier callipers. All the four materials employed i.e., ABS, PLA, PP, and PET displayed greater precision along the X and Y axes excluding the Z axis [19]. A CAD model provides nominal dimensions, while an FDM model provides real dimensions. The average values of actual dimensions were used to determine the exact dimensions of the samples. Water absorption tests were conducted on uncoated and coated PLA specimens as per ASTM D570-98. Even without surface treatments, LVL1 sample consumes more moisture per area than LVL2, regardless of whether protective coatings are applied [20]. Shells, print temperature, infill and printing style are controllable printing characteristics that impact DA [21]. $C_{10}H_{30}O_5Si_5$, SiO_2 nanoparticles (R812S), $(C_2H_6OSi)_n$ (BP-9400) and a nonionic surface-active agent are included in this combination (Triton X-100). When a modified varnish coated onto a Pineapple peel fiber (PAPF) bio-composite with a weight percentage of modifying agents larger than 101.87 percent was used, the water contact angle was lowered [22]. Long-term dimensional instability could decrease the accuracy of samples. FDM was used to create 3D objects using industrial thermoplastics like ABS. Variations in the dimensions were less than 0.1%. However, moisture absorption led to dimensional uncertainty in some polymers, such as polyamides [23].

Average length and width were used to obtain an original value for the object using a 0.001 mm accurate digital micrometer [24]. The morphology of AZO surfaces obtained in AFM was remarkably consistent with that of SEM [25]. Chitin hydrogels made with 3% LiCl exhibited low viscosity and viscous behaviour. Hydrogels that resulted from the 10% LiCl preparation had a softer structure and poor mechanical characteristics because of the chitin segments that have accumulated on the hydrogel surface [26]. Chitosan-based nanoparticles were spray-coated onto silicon wafers to create superhydrophobic surfaces [27]. There was a higher contact angle (77-79°) when the Ca-O-P gel was applied in layers 1 and 5 to a substrate coated with the gel. With 15 dips, the specimen exhibited the highest contact angle (87°). With 30 dipping times, the surface's contact angle decreased to 75° [28]. In all microchannel surfaces coated with TiO_2-HTMS, superhydrophobic states were achieved, with contact angles greater than 160° [29]. Longer soaking time in the chitosan solution reduced the hydrophobicity of the modified scaffold signifying more macromolecules on the PLA surface. The 3D printed PLA scaffold coated with $Ca_{10}(PO_4)_6(OH)_2$-chitosan was found to be hydrophilic based on the contact angle [30].

Hydrophobic and injectable properties can be achieved with polyesters and PCs derived from lactic acid, glycolic acid, caprolactone, and diol [31]. A rough surface was found on a 3D printed low-resolution mould manufactured with 143° WCA and 36.42 µm roughness [32]. To better prominent differences in surface energy between spray-coated PVA and PTFE supports, an intermediate polymer layer was not needed [33]. As a result of the excellent interface interaction between ACNTB-SiO_2-KH570 and superior strength-toughness combination, the composite coating exhibited excellent mechanical durability, super-hydrophobicity and excellent adhesion to various substrates [34]. The superhydrophobic coatings developed with outstanding mechanical stability and self-healing ability allowed them to be considerably more dependable and endure longer in harsh situations [35]. Coating polyester fabric with FD-POSS and FAS resulted in a super-hydrophobic and super-oleophobic surface [36]. Combined with proper surface topography, Coatings polymerized with plasma and with proper surface topography imparting hydrophobicity or superhydrophobicity can be applied to any kind of material [37]. Surface wettability was assessed using the CA in ambient air. A droplet of pristine water (5L) was deposited on the surface of the specimen at a temperature of 20°C [38]. Hydroxyapatite, brushite, octa calcium phosphate,

and hydroxyapatite are the mineral mixtures in the hydrogel/CP coating layers [39]. Process parameters on forming quality have been extensively researched. In most cases, these coatings contain precious ingredients like Ag and fluorine-containing compounds that are regarded as harmful to the environment. Therefore, creating smart, responsive hydrophobic coatings using environmentally friendly, low-cost ingredients has become an inevitable trend. Various chemical concentrations on the surface of printed items must be investigated concerning surface wettability and water absorption when coatings are used. Among functional materials, chitin and tricalcium phosphate possess excellent properties such as biocompatibility, biodegradability, and non-toxicity.

In this research, the synthesis of hydrophobic coatings using tricalcium phosphate-chitin chemicals is demonstrated. A standard FDM 3D printer was employed to print different ABS specimens which were then dipped in the synthesized solution. To get clear solutions, trials were conducted on tricalcium phosphate-chitin combinations. Various concentrations of concentrated solutions were applied to samples and their effects were investigated on surface roughness and dimensional accuracy. Water absorbed by the coated specimens was calculated. A profilometer was used to measure SR, and a vernier calliper was used for DA measurement. Surface coatings were tested for static contact angle using contact angle measurement equipment, as well as the wettability variations of 3D printed specimens. Employing various Tricalcium phosphate-chitin compositions, research focused on evaluating the hydrophobic nature of coatings on 3D printed specimens.

2. Methodology

2.1 Materials

ABS filament was employed for layer fabricating test specimens whereas for the synthesis of solutions and coating, following were used - Chitin purified [Make: OTTO], Tricalcium phosphate extra purified [Make: OTTO, (MW= 310.18 g mol-1)], HCL [99%] [Make: AVRA], Acetic Acid [Make: Zen Chemicals,99%], sulfuric acid [Make: Research Labs], NaOH [Make: Research Labs, NaOH in pallets], DMAc [Make: SDFCL], LiCl [Make: SDFCL], isopropyl alcohol [Make: SDFCL]

2.2 Design of Samples

Initially, three test specimens were designed using CATIA software and converted into STL files. These are - a square block measuring 31.5x31.5x4.5 mm; a BCC structure measuring 31.5x31.5x4.5 mm with square pores of 1.5x1.5 mm; and a BCC structure with top and bottom plates measuring 31.5x 31.5x4.5 mm and 31.5x31.5x1 mm respectively, with square holes measuring 1.5x1.5 mm. Fig. 1 shows CAD images of test samples.

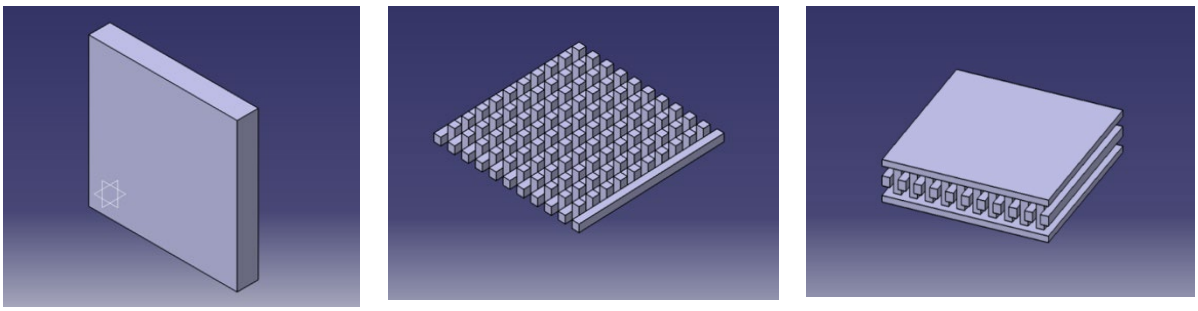

(a) (b) (c)

Fig. 1 - CAD models (a) a square block with hexagonal infill; (b) a BCC structure and; (c) a BCC structure with top and bottom plate

Table 1 - Characteristics of ABS printing materials

Material	ABS	**Color**	Black
Brand		**Density**	1.04g/cm3
Diameter	1.75mm	**Printing temperature**	220-250℃
Melting point temperature	220℃	**Flow rate**	2-4g/10 min

Table 2 - Specimen identification

Samples	3D printed specimens
1	BCC Structure
2	Square Block
3	Top and Bottom along the structure
4	Top and Bottom along the structure with supports

2.3 3D Printing of Test Samples

A Flash Forge Dreamer 3D printer based on FDM technology was used to print the test specimens as demonstrated in Fig. 2 (a) and Fig. 2 (b). To slice the STL file and print the solid model, Flash print software was employed for selecting print settings and slicing the STL file. Characteristics of ABS material are presented in Table 1 whereas Table 2 displays the specimen identification. Specimens were 3D printed according to the parameters indicated in Table 3. Default parameters were selected for other process variables. 3D printed specimens are exhibited in Fig. 3. Post-processing involved removing dust and other contaminants with concentrated isopropyl alcohol after printing.

Table 3 - Printing parameters

Specimens	Layer thickness (mm)	Infill (%)	No. of shells	Infill type	Support structure
1	0.15	0	2	-	With supports
2	0.15	20	2	Hexagonal	-
3	0.15	20	2	Hexagonal	With supports
4	0.15	20	2	Hexagonal	Without supports

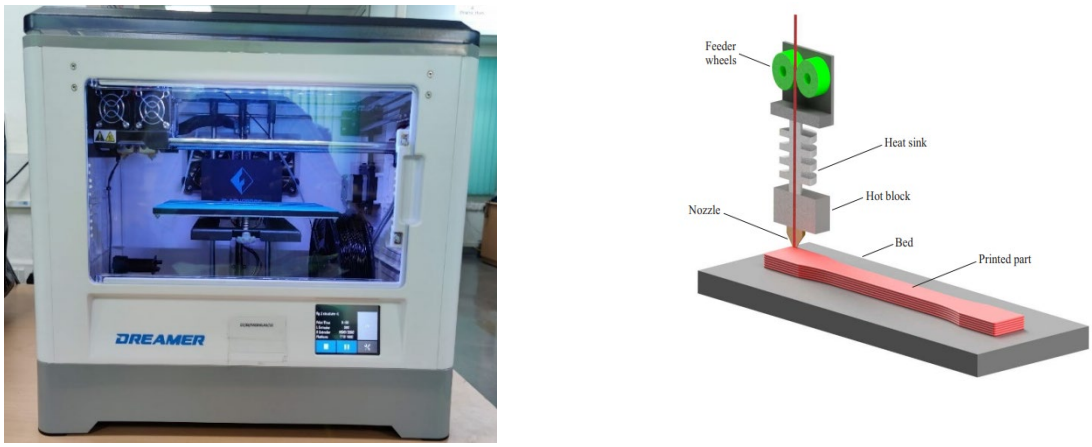

(a) (b)

Fig. 2 - FDM printing (a) 3D printer used; (b) schematic illustration of the FDM process

3. Synthesis of Surface Coatings

Surface coatings were produced by a concoction of Tricalcium phosphate-chitin solutions with ratios of 70:30.

3.1 Preparation of Tricalcium Phosphate Solution

A clear Tricalcium phosphate solution was achieved by adopting the following approach.

- Solution 1 was prepared by adding 10 g, and 20 g of tricalcium phosphate dissolved in water and made up to 100mL with stirring. After 24 hours, it was observed that tricalcium phosphate was not completely dissolved. Hence solution 1 was discarded.
- Solution 2 was prepared by adding 4 g, 6 g, 8 g, and 10 g of tricalcium phosphate to 3 ml, 5 ml, 7 ml, and 10 ml HCl and made up to 100 ml with distilled water. Solution 2 was also discarded due to lack of clarity and transparency even after 24 hours of dissolution, attributing to the non-dissolution of tricalcium phosphate.
- Solution 3 was prepared by adding 3 g of tricalcium phosphate to 3 ml HCl and made up to 100 ml. After 24 hours Tricalcium phosphate was partially dissolved, hence solution 3 was discarded. For solutions 2 and 3 HCl drops (15-20) were added and stirred to achieve a clear solution.
- Solution 4 was prepared to determine the exact proportions of HCl necessary to get a clear solution. The addition of tricalcium phosphate at different weights of 4 g, 6 g, 8 g, 10 g to 6 ml, 8 ml, 10 ml, and 12 ml HCl respectively and made up to 100 ml. At ambient temperature, this mixture was agitated for 30 minutes at 1600 rpm. After 24 hours, solutions containing 4 g and 6 g of tricalcium phosphate, were observed clear and 8 g and 10 g were partly cloudy. Hence solution 4, with tricalcium phosphate of 4g and 6g solutions was selected for surface coatings.

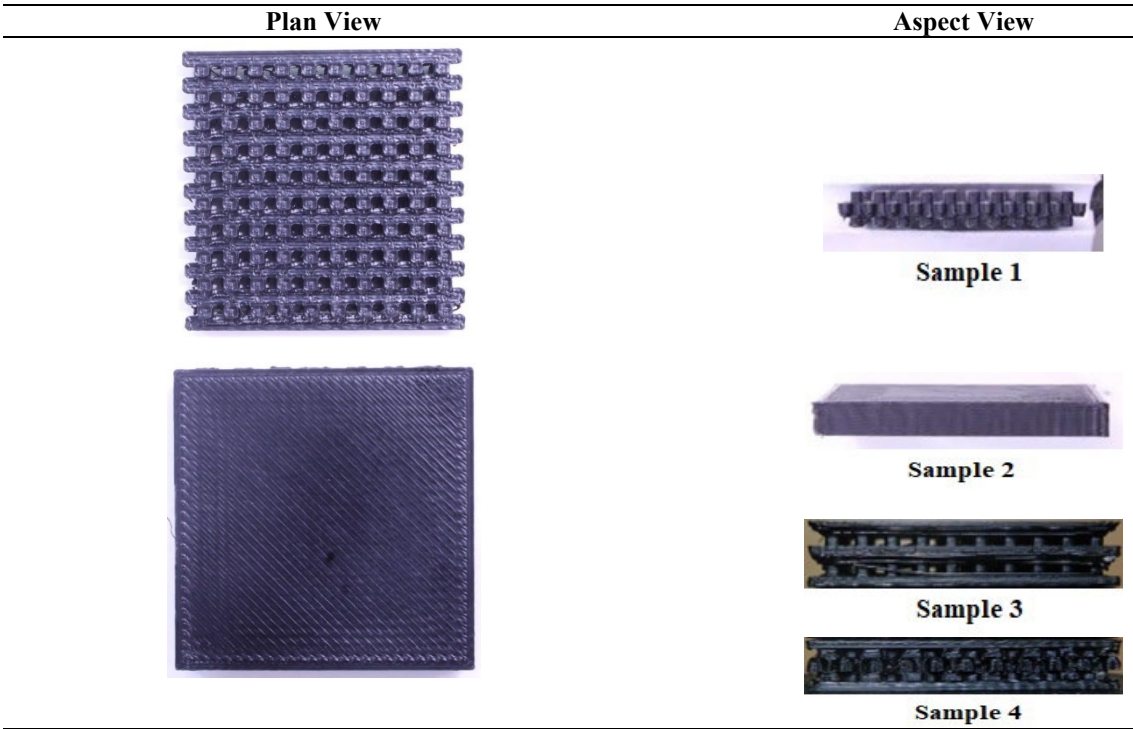

Fig. 3 - 3D printed samples

3.2 Preparation of Chitin Solution

Chitin's clear solution was made as follows:

- Solution 1 was prepared by the addition of 0.6 g of chitin to 3 ml acetic acid and made up to 100 ml with stirring. After 24 hours it was observed that chitin was not completely dissolved. Hence solution 1 was discarded.
- Solution 2 was prepared by adding 0.6 g of chitin to 6 ml HCl and made up to 100 ml. Solution 2 was also discarded due to lack of clarity and transparency even after 24 hours of dissolution, attributing to the non-dissolution of chitin.
- Solution 3 was prepared by the addition of 0.6 g of chitin to 2 ml of sulphuric acid and made up to 100 ml with stirring. After 24 hours, it was observed that chitin was not completely dissolved. Hence solution 3 was discarded.
- Solution 4 was prepared by the addition of 0.6 g of chitin to 6 ml acetic acid and made up to 100 ml. The mixture was swirled for one hour at ambient temperature at 1500 rpm and sonicated for 30 minutes. After 24 hours, it was observed that chitin was not completely dissolved. Hence solution 4 was discarded.
- Solution 5 was prepared by the addition of 0.3 g of chitin to 1g of LiCl of 30 ml DMAc. A stirring speed of 1600 rpm was used for 3 hours at room temperature. After 24 hours, centrifugate the mixture for 10 minutes at 2500 rpm to remove precipitates, and a clear solution was observed.
- Solution 6 was formulated by adding 0.3 g of chitin to 0.5 g of LiCl of 15 ml DMAC to that 10 ml acetic acid. The blend was stirred at room temperature for 3 hours at 1600 rpm. After 24 hours, centrifugate the mixture for 10 minutes at 2500 rpm to remove precipitates, and a clear solution was observed. Hence solutions 5 and 6 were selected for surface coating.

3.3 Preparing Surface Coating

Chemical proportions of tricalcium phosphate solution are exhibited in Table 4 (a) and the chemical constitution of chitin solution is displayed in Table 4 (b). The weightage of chemical quantities used for the preparation of 30ml solution of 70:30 ratios is shown in Table 5. The solutions are stirred for 10 minutes at 2500 rpm using a magnetic stirrer at room temperature.

Table 4 (a) - Tricalcium phosphate solution chemical proportions

	$Ca_3(PO_4)_2$ (g)	HCl (ml)	Distilled water (ml)
A_1	4	6	96
A_2	6	8	94

Table 4 (b) - Chitin solution chemical composition

	$(C_8H_{13}O_5N)_n$ (g)	LiCl (g)	DMAc (ml)	Acetic acid (ml)
B_1	0.3	1	30	-
B_2	0.3	0.5	15	10

Table 5 - Tricalcium phosphate - chitin solution concentration proportions

	Composition of Tricalcium phosphate- Chitin solutions	Ratios
Solution 1	A_1: B_1	
Solution 2	A_1: B_2	
Solution 3	A_2: B_1	21:9
Solution 4	A_2: B_2	

3.4 pH Level Measurement

For hydrophobic surfaces, the pH level must be 7 or higher [42]. pH levels of solutions were measured using Elico LI 120 pH meter. Through the agitation process, 5M of NaOH solution was added until pH value of 7 was achieved. An illustration of the difference in pH level responses before and after adding aqueous NaOH can be found in Table 6. Graphs of pH level responses for day-to-day variations in solutions are exhibited in Fig. 4. Initially, the pH levels of samples were ≤1.5, but dropped very rapidly after titration with NaOH solution. After 24 hours, the fluid was spun at 2500 rpm for 10 minutes. Consequently, a clear solution was reached. The precipitates were added to 100 ml distilled water and mixed, then phenolphthalein was added. The solution turned pink, indicating that the precipitates are NaOH. The pH of the solutions was ≤ 8 on day 2 and after day 2 were close to pH 7.

Table 6 - pH level responses

Solutions	Initial pH level	pH level after titration	After centrifugation		
			Day 2 pH level	Day 3 pH level	Day 4 pH level
1	1.37	8.01	7.93	7.92	7.9
2	1.19	7.01	7.01	6.99	6.99
3	1.50	7.52	7.5	6.92	6.90
4	1.22	7.04	7.0	6.97	6.96

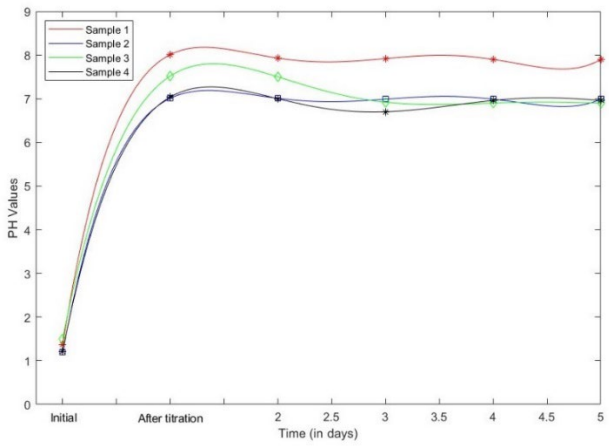

Fig. 4 - Variations in pH level responses in solutions

3.5 Surface coating of 3D Printed samples

Four 3D printed specimens were dipped in the synthesized solutions for applying the coating. 3D printed samples were dip coated for 60 minutes, and then left to dry at ambient temperature for 24 hours. The mapping of 3D printed specimens and their immersing solutions is given in Table 7 whereas the immersion process is depicted in Fig. 5.

Table 7 - 3D printed specimens are immersed in solutions

Solutions	3D printed samples
Solution 1	1
Solution 2	2
Solution 3	3
Solution 4	4

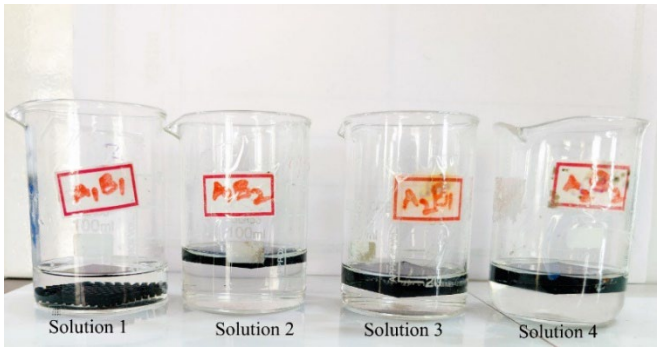

Fig. 5 - 3D printed specimens immersed in solutions

4. Measurements

4.1 Dimensional Accuracy

Dimensional accuracy (DA) was determined by measuring 3D printed specimens and comparing them with the CAD models. 3D printed specimens were measured using Digital Vernier Calipers (Make: Mitutoyo, 150 mm). Measurements were recorded at three locations on each of the specimens pre and post-coating. Error and percentage error were estimated as per equations 1 and 2 respectively.

$$\text{Error or Difference} = \text{Measured value} - \text{Design value} \quad (1)$$

$$\%\ \text{Error} = \frac{/\text{error or diiference}/}{\text{Average}}] \times 100 \quad (2)$$

4.2 Surface Roughness and Weight Measurement

Surface roughness tester SJ410 (Make: Mitutoyo, simple column stands) was utilized to measure the average surface roughness of untreated and treated 3D printed specimens with a cutoff length (λ_c) of 0.8 mm. Three different spots were analyzed on the surface of each specimen. In this research, roughness values (Ra) are averaged, and observations are normalized to the deposition direction. Three measurements were taken on each specimen to avoid errors in the measurement. Surface roughness was gauged at the same site pre and post-coating.

A digital weighing machine (Model: Shimadzu ATX224) with a reading of 0.0001 g was employed for estimating the mass of the specimens. An average of three weight measurements was taken for each sample before and after coating. Percentage deviation in weight and surface roughness was computed as per equation 3 [9].

$$\text{Percent change} == \frac{/\text{Error}/}{\text{Average}} \quad (3)$$

4.3 Surface Wettability

Surface wettability was measured using the water droplet contact angle technique. As per water contact angle (WCA), wetting behavior can be grouped into four regimes. WCAs between $10° < \theta < 90°$ indicate a hydrophilic regime and those between $90° < \theta < 150°$ indicate a hydrophobic regime. Superhydrophilicity is when the WCA < 10° in less than 1s from initial wetting. On the other hand, WCAs > 150° indicate super hydrophobicity [40]. A goniometer (DSA25 with the temperature-controlled chamber, KRUSS, Germany) was utilized for contact angle measurement of droplets post-coating. Analysis of droplets was carried out using KYOWA's FAMAS (Interface Measurement and Analysis System). CA average was calculated by analyzing water droplet size of 2µL at two different spots on each specimen's surface.

4.4 Water Absorption

Water absorption assessments were accomplished as per ASTM D570-98 to monitor size and weight changes. Water immersion tests were performed at room temperature on each specimen before and after weighing. To ensure that water

reached the base of the specimens, the base was covered with filter paper designed to soak up water. Weighing of samples was carried out at 30 minutes' intervals in the initial 4 hours, followed by 1-hour intervals in the next 4 hours, then every 24 hours, and finally every 24 hours for the next 2 days. Samples were immersed for 48 hours in water. Equation 4 estimates weight gain (WG) and equation 5 porosity [20].

$$WG = \frac{m_{sat} - m_{dry}}{m_{dry}} \times 100\ \% \quad (4)$$

$$P = \frac{(m_{sat} - m_{dry})/\rho H2O}{V} \times 100\ \% \quad (5)$$

Weight gain per unit area can be calculated using equation 6. A saturated mass (m_{sat}) is the mass after a test, a dry mass (m_{dry}) is the initial mass of an experiment, and V is the sample volume. ρ_{H2O} is water density i.e., 1 g/cm^3. Absorption coefficient (K) was computed graphically where in x-axis depicts the root of the dipping period and the y-axis WG per unit area of 3D printed specimens [20].

$$\frac{WG}{area} = \frac{m_{wet} - m_{dry}}{A \times m_{dry}} \quad (6)$$

A is the area of one of the faces of the specimen, and m_{wet} represents the mass of the specimen at a particular instant.

5. Results and Discussions

5.1 Dimensional Accuracy

In FDM, nominal dimensions are generated from CAD models while actual dimensions are derived from FDM printed models. The average values of actual dimensions are measured to know the accurate dimension of the samples. The dimensions of 3D printed specimens were calculated using equations 2 and 3 are illustrated in Table 8. The dimensional accuracy plot across axes is portrayed in Fig. 6. In sample 1, there is an average difference of 0.05 mm, 0.15 mm and 0.03 mm along the x, y and z axes respectively. There is accuracy of 0.158%, 0.477% and 0.662% at x, y and z axes respectively. Sample 2 has an average difference of 0.09 mm, 0.14 mm and 0.033 mm along x, y and z axes respectively. Dimensions are approximately 0.223%, 0.44% and 0.735% accurate at the x, y and z axes respectively. Samples 3 and 4 have an average difference of 0.03 mm, 0.02 mm and 0.036 mm along the x, y and z axes respectively. There is accuracy of 0.063% on the x-axis, 0.116% on the y-axis, and 0.459% on the z-axis. Since an ultra-thin coating was laid on the specimens, the differences in dimensions between coated and uncoated samples are minimal. A high-accuracy CMM was used to determine the difference between coated and uncoated surfaces.

Table 8 - Dimensional accuracy of the 3D printed specimens

Specimens		Nominal value (mm)	Actual Value (mm)			Average of actual values (mm)	Difference (mm)	Dimensional accuracy (%)
			1	2	3			
	x	31.5	31.56	31.54	31.55	31.55	0.05	0.158
1	y	31.5	31.35	31.34	31.36	31.35	0.15	0.477
	z	4.5	4.54	4.53	4.52	4.53	0.03	0.662
	x	31.5	31.4	31.41	31.42	31.41	0.09	0.23
2	y	31.5	31.35	31.37	31.36	31.36	0.14	0.44
	z	4.5	4.55	4.52	4.53	4.53	0.033	0.735
	x	31.5	31.49	31.48	31.47	31.48	0.02	0.063
3	y	31.5	31.56	31.53	31.52	31.53	0.036	0.116
	z	6.5	6.54	6.53	6.52	6.53	0.03	0.459
	x	31.5	31.49	31.48	31.47	31.48	0.02	0.063
4	y	31.5	31.56	31.53	31.52	31.53	0.036	0.116
	z	6.5	6.54	6.53	6.52	6.53	0.03	0.459

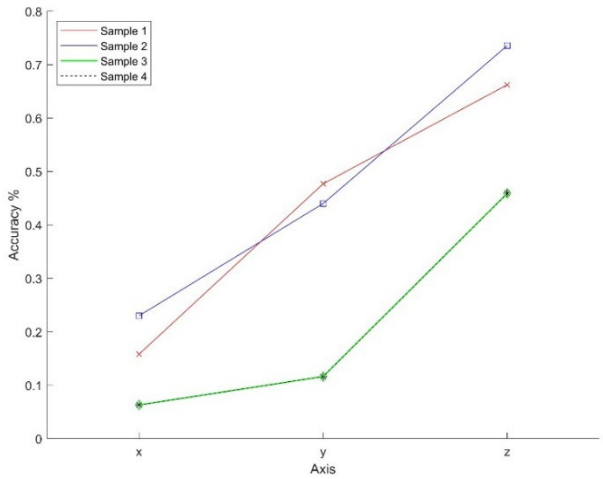

Fig. 6 - Dimensional accuracy plot across axes

5.2 Surface Roughness and Weight Measurement

Table 9 and Fig. 7 (a) and (b) represents the average SR of printed specimens - coated and uncoated as well as the percentage difference between them. Uncoated specimens were observed with higher surface roughness (Ra) as compared to coated specimens. Specimen S2 had the highest surface roughness, followed by specimens S3 and S4. It is reported that layer thickness and filling process considerably affect the surface roughness of 3D printed components [42]. Coatings significantly reduced the roughness of 3D printed specimens (by over 50% for specimens S2 and S3, and by over 30% for specimen S4) mainly due to varied compositions of coatings. Due to solution 3, surface-coated specimen S2 has a 51.39 % difference, while specimen S3 has a 68.84 % difference. There was a 39.168 % reduction in the SR of specimen S4. Smoothing the surface of 3D printed objects is frequently made simpler by coatings having a larger solid content [41].

Table 9 - Average SR values of 3D printed specimens before and after coating

	S2	S3	S4
Before coating (µm)	6.30	2.95	2.93
After coating (µm)	3.72	1.44	1.97
Percentage (%)	51.39	68.84	39.16

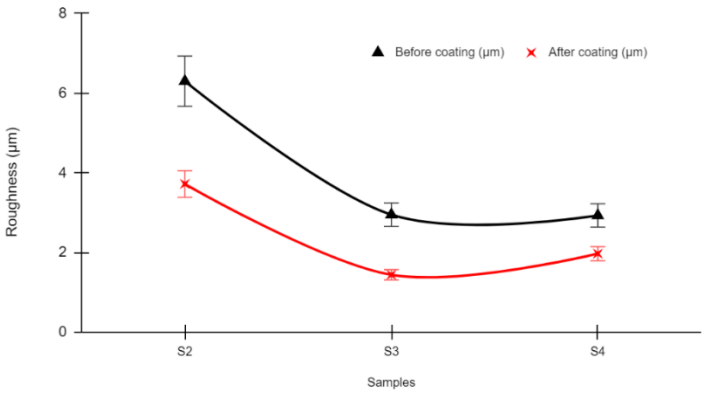

Fig. 7 (a) - Mean surface roughness of 3D printed samples pre and post coating

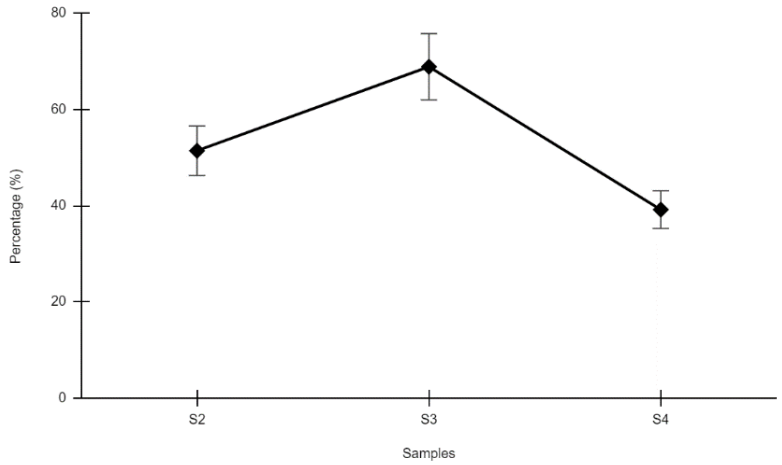

Fig. 7 (b) - Percentage reduction in surface roughness of 3D printed samples pre and post coating

SR profiles of printed samples pre and post-coating are portrayed in Fig. 8. The crests and valleys caused by layered deposition are visibly clear as rough surfaces before coating in specimens. Surfaces of 3D printed samples are smoothened after immersion due to the laying of a thin coating on their surfaces. Surface profilometer measurement graphs showed high peak points and more fluctuations in specimens before coating. A slight reduction in surface roughness is observed post coating as the peak heights are significantly reduced resulting in a smooth surface of the coated 3D printed samples

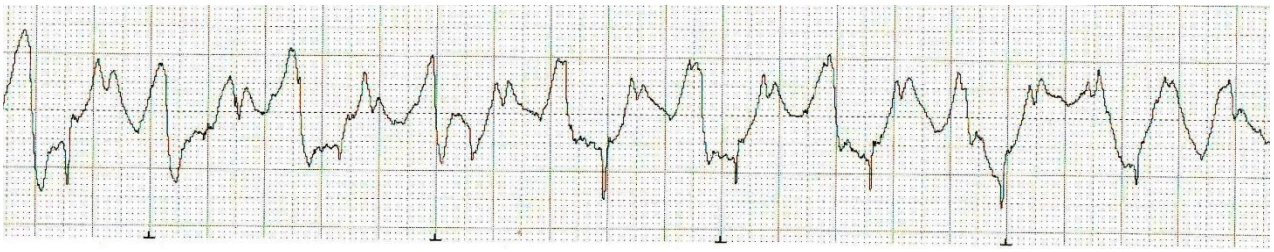

(a)

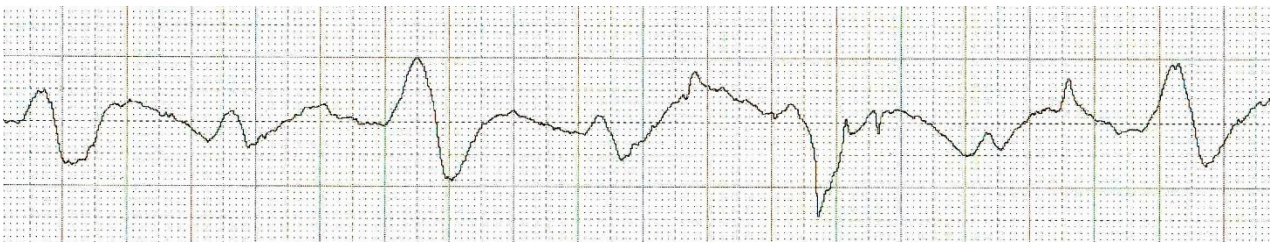

(b)

Fig. 8 - Surface roughness profiles of 3D printed specimen (a) pre-coating; (b) post-coating

5.3 Surface Wettability

The prime intent of this exploration focused on determining the feasibility of forming a hydrophobic coating on the 3D printed ABS specimens. Fig. 9 depicts the images of surface wettability tests performed on these specimens. Solution 1 coated specimen i.e., sample 1 exhibited a maximum contact angle of 109.3°. The average contact angle for solution 2 coated specimen i.e., sample 2 was 95.85°. In the case of solution 3 coated specimen i.e., sample 3, the average contact angle was found to be 99.69° whereas, in solution 4 specimen i.e., sample 4, it was 95.8°. Results consolidated the formation of hydrophobic surfaces of layered deposition samples dipped in different solutions. However, the coating formed was observed to be only hydrophobic and not superhydrophobic as the maximum contact angle is below 150°.

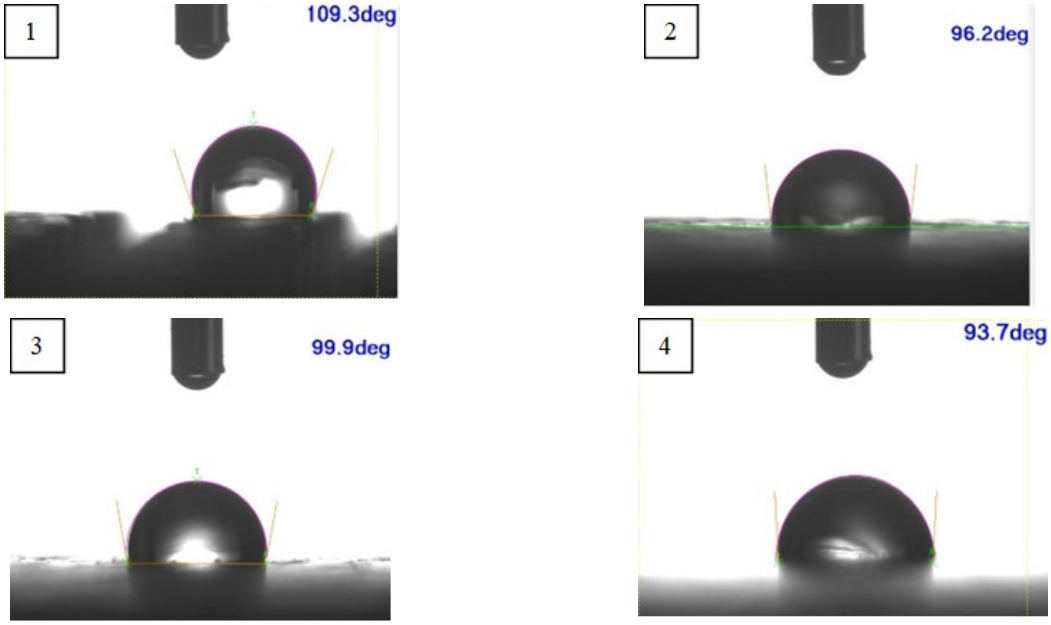

Fig. 9 - Surface wettability test on samples

5.4 Water Absorption

Table 10, Fig. 10 and Fig. 11 exhibit the outcomes of the water absorption test conducted on the 3D printed specimens. As per the averages, the maximum weight gained in 3D printed coated specimens are 21.636 x 10^{-5} g for sample 1, 6.49 x 10^{-5} g for sample 2, 1.83x10^{-4} g for sample 3, and 14.40 x 10^{-5} g for sample 4 respectively. Coated specimens represented variation in water absorption to an extent of 15%. Specimen coated with solution 1 depicted a reduction of 21.46737 %. Specimen coated with solution 3 absorbed more water per area than sample 1. This could be attributed to the presence of microcracks which are formed due to the temperature at which the polymer is processed [21].

Table 10 - Water absorption results on 3D printed specimens post coating

Samples	1	2	3	4
WG%	21.46737	6.441698	18.1557155	14.25564
p	0.009736	0.003219	0.011415	0.009973
WG/A	21.636 x 10^{-5}	6.49 x 10^{-5}	1.83x10^{-4}	14.40 x 10^{-5}

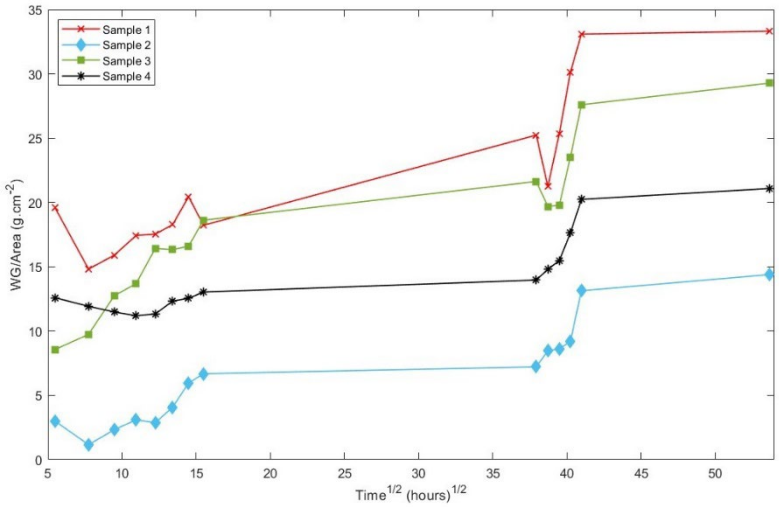

Fig. 10 - Evolution of weight gain per area for 3D printed samples after coating

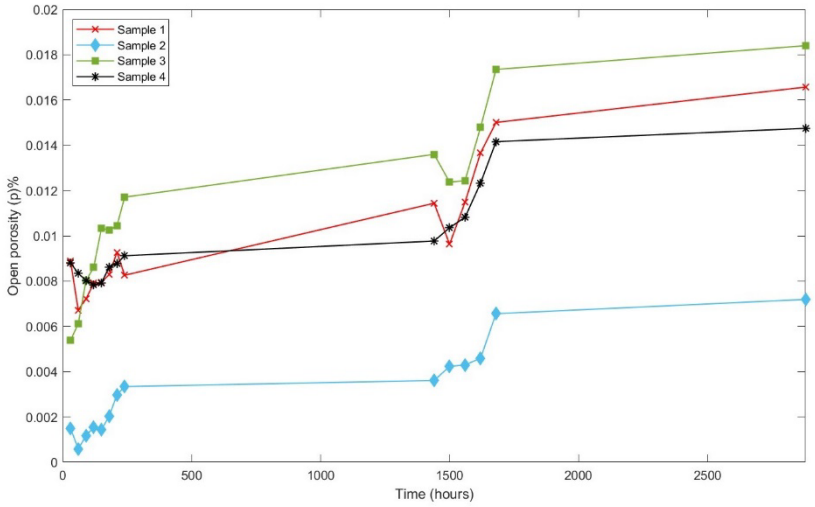

Fig. 11 - Evolution of open porosity of 3D printed samples after coating

6. Conclusions

The fabrication, characterization, and synthesis of surface coatings on 3D printed ABS specimens are presented. In the development of surface coating, a 30mL solution of tricalcium phosphate-chitin solution with varying weight per volume was utilized. The dip coating process was employed successfully for creating a hydrophobic coating, considerably improving the hydrophobicity of ABS specimens. Because of the ultra-thin surface coating, insignificant variation was noticed in the dimensional accuracy of pre and post-coated 3D printed samples. The laying of coating on the 3D printed samples resulted in decreasing the surface roughness. It was found that the surface wettability for solution 1 has a contact angle of 109.3^{o} when compared to solution 2, solution 3 and solution 4. The remaining solutions exhibited contact angle $\leq 90^{o}$. The proportion of weight gain due to water absorption was considerably low for square blocks. Application of developed solutions on 3D printed ABS specimens resulted in a formation of a hydrophobic coating. Hydrophobic surface coatings developed will be further investigated using scanning electron microscopy.

Acknowledgement

The authors appreciate and recognize the support rendered by the staff of Additive Manufacturing laboratory, Chemistry Laboratory and Center for Nanotechnology, VNRVJIET Hyderabad and ARCI Hyderabad for permitting to use of their facilities for study, data collection and analysis.

References

[1] Poornaganti, S., Yeole, S. N., & Kode, J. P. (2022). “Insights on surface characterization of 3D printed polymeric parts”. *Materials Today: Proceedings*.

[2] Lee, K. M., Park, H., Kim, J., & Chun, D. M. (2019). “Fabrication of a superhydrophobic surface using a fused deposition modeling (FDM) 3D printer with poly lactic acid (PLA) filament and dip coating with silica nanoparticles”. *Applied Surface Science*, *467*, 979-991.

[3] Yang, Huadong, Fengchao Ji, Zhen Li, and Shuai Tao. "Preparation of hydrophobic surface on PLA and ABS by fused deposition modeling." Polymers 12, no. 7 (2020): 1539.

[4] Pradhan, S. R., Singh, R., Banwait, S. S., Puhal, M. S., Singh, S., & Anand, A. (2021). “A comparative study on investment casting of dental crowns for veterinary dentistry by using ABS patterns with and without wax coating.” In *E3S Web of Conferences* (Vol. 309). EDP Sciences.

[5] Mura, A., Adamo, F., Wang, H., Leong, W. S., Ji, X., & Kong, J. (2019). “Investigation about tribological behavior of ABS and PC-ABS polymers coated with graphene.” *Tribology International*, *134*, 335-340.

[6] Chen, W., Nichols, L., Brinkley, F., Bohna, K., Tian, W., Priddy, M. W., & Priddy, L. B. (2021). “Alkali treatment facilitates functional nano-hydroxyapatite coating of 3D printed polylactic acid scaffolds”. *Materials Science and Engineering: C*, *120*, 111686.

[7] Kowalczyk, P., Trzaskowska, P., Łojszczyk, I., Podgórski, R., & Ciach, T. (2019). “Production of 3D printed polylactide scaffolds with surface grafted hydrogel coatings.” *Colloids and Surfaces B: Biointerfaces*, *179*, 136-142.

[8] Chen, W., Nichols, L., Brinkley, F., Bohna, K., Tian, W., Priddy, M. W., & Priddy, L. B. (2021). “Alkali treatment facilitates functional nano-hydroxyapatite coating of 3D printed polylactic acid scaffolds”. *Materials Science and Engineering: C*, *120*, 111686.

[9] Chohan, J.S., Kumar, R., Singh, T.B., Singh, S., Sharma, S., Singh, J., Mia, M., Pimenov, D.Y., Chattopadhyaya, S., Dwivedi, S.P. and Kapłonek, W., 2020. "Taguchi S/N and TOPSIS based optimization of fused deposition modelling and vapor finishing process for manufacturing of ABS plastic parts." *Materials*, *13*(22), p.5176.
[10] Khosravani, M. R., Schüürmann, J., Berto, F., & Reinicke, T. (2021). "On the post-processing of 3d-printed abs parts." *Polymers*, *13*(10), 1559.
[11] Omar, M. F. M., Sharif, S., Ibrahim, M., Hehsan, H., Busari, M. N. M., & Hafsa, M. N. (2012). "Evaluation of direct rapid prototyping pattern for investment casting." In *Advanced Materials Research* (Vol. 463, pp. 226-233). Trans Tech Publications Ltd.
[12] Haidiezul, A. H. M., Aiman, A. F., & Bakar, B. (2018, March). "Surface finish effects using coating method on 3D printing (FDM) parts". In *IOP Conference Series: Materials Science and Engineering* (Vol. 318, No. 1, p. 012065). IOP Publishing.
[13] Sierra, J., Villa, D. S., Velasquez, A. M., & Villaneda, W. (2020). "Relation Between Mechanical Properties and 3D Printer Configurations Parameters Using PLA at Open-Source Prusa I3". *International Journal of Integrated Engineering*, *12*(8), 97-108.
[14] Chai, Y., Li, R. W., Perriman, D. M., Chen, S., Qin, Q. H., & Smith, P. N. (2018). "Laser polishing of thermoplastics fabricated using fused deposition modelling". *The International Journal of Advanced Manufacturing Technology*, *96*(9), 4295-4302.
[15] Garg, A., Bhattacharya, A., & Batish, A. (2017). "Chemical vapor treatment of ABS parts built by FDM: Analysis of surface finish and mechanical strength." *The International Journal of Advanced Manufacturing Technology*, *89*(5), 2175-2191.
[16] Winkler, H., Heins, M., & Nyhuis, P. (2007). "A controlling system based on cause-effect relationships for the ramp-up of production systems". *Production Engineering*, *1*(1), 103-111.
[17] Ali, Hafiz Muhammad, Muhammad Arslan Qasim, Sullahuddin Malik, and Ghulam Murtaza. "Techniques for the fabrication of super-hydrophobic surfaces and their heat transfer applications." Heat Transf. Models Methods Appl 1 (2018): 283-315.
[18] Wang, Zehao, Li Yuan, Guozheng Liang, and Aijuan Gu. "Mechanically durable and self-healing superhydrophobic coating with hierarchically structured KH570 modified SiO2-decorated aligned carbon nanotube bundles." Chemical Engineering Journal 408 (2021): 127263.
[19] Hasan, Sakib Mohammad, Toni Ivanov, Dragoljub Tanović, Aleksandar Simonović, and Miloš Vorkapić. "Dimensional accuracy and experimental investigation on tensile behavior of various 3D printed materials." In 9th International Scientific Conference on Defensive Technologies, OTEH 2020, October 15-16, Belgrade, Serbia, pp. 400-406. The Military Technical Institute, Belgrade, Serbia, 2020.
[20] Vicente, Carlos, João Fernandes, Augusto Deus, Maria Vaz, Marco Leite, and Luis Reis. "Effect of protective coatings on the water absorption and mechanical properties of 3D printed PLA." Frattura ed Integrità Strutturale 13, no. 48 (2019): 748-756.
[21] Aslani, Kyriaki-Evangelia, Konstantinos Kitsakis, John D. Kechagias, Nikolaos M. Vaxevanidis, and Dimitrios E. Manolakos. "On the application of grey Taguchi method for benchmarking the dimensional accuracy of the PLA fused filament fabrication process." SN Applied Sciences 2, no. 6 (2020): 1-11.
[22] Tarmizi, Z. I., Maski, A. N., Ali, R. R., Jusoh, N. W. C., Akim, A. M., Eshak, Z., ... & Ibrahim, N. (2019). "Fabrication of hydrophilic silica coating varnish on pineapple peel fiber based biocomposite". *International Journal of Integrated Engineering*, *11*(7), 77-82.
[23] Queral, V., E. Rincón, V. Mirones, L. Rios, and S. Cabrera. "Dimensional accuracy of additively manufactured structures for modular coil windings of stellarators." Fusion engineering and design 124 (2017): 173-178.
[24] Unkovskiy, Alexey, Phan Hai-Binh Bui, Choursistine Schille, Juergen Geis-Gerstorfer, Fabian Huettig, and Sebastian Spintzyk. "Objects build orientation, positioning, and curing influence dimensional accuracy and flexural properties of stereolithographically printed resin." Dental Materials 34, no. 12 (2018): e324-e333.
[25] Valerini, Daniele, Loredana Tammaro, Fulvia Villani, Antonella Rizzo, Ivana Caputo, Gaetana Paolella, and Giovanni Vigliotta. "Antibacterial Al-doped ZnO coatings on PLA films." Journal of Materials Science 55, no. 11 (2020): 4830-4847.
[26] Nguyen, K. D., & Kobayashi, T. (2020). "Chitin hydrogels prepared at various lithium chloride/n, n-dimethylacetamide solutions by water vapor-induced phase inversion". *Journal of Chemistry*, *2020*.
[27] Wang, S., Sha, J., Wang, W., Qin, C., Li, W., & Qin, C. (2018). "Superhydrophobic surfaces generated by one-pot spray-coating of chitosan-based nanoparticles". *Carbohydrate polymers*, *195*, 39-44.
[28] Beganskiene, A., Stankeviciute, Z., Malakauskaite, M., Bogdanoviciene, I., Mikli, V., Tõnsuaadu, K., & Kareiva, A. (2013). "Sol-Gel Approach to the Calcium Phosphate Nanocomposites". *Nanostructured Materials and Nanotechnology VII*, 1-13.
[29] Barraza, B., Olate-Moya, F., Montecinos, G., Ortega, J. H., Rosenkranz, A., Tamburrino, A., & Palza, H. (2022). "Superhydrophobic SLA 3D printed materials modified with nanoparticles biomimicking the hierarchical structure of a rice leaf." *Science and Technology of Advanced Materials*, *23*(1), 300-321.

[30] Wang, J., Nor Hidayah, Z., Razak, S. I. A., Kadir, M. R. A., Nayan, N. H. M., Li, Y., & Amin, K. A. M. (2019). "Surface entrapment of chitosan on 3D printed polylactic acid scaffold and its biomimetic growth of hydroxyapatite". *Composite Interfaces*, *26*(5), 465-478.
[31] Wulandari, A. F., Zulaihah, S., Rachmadanti, I., & Aminatun. (2020, December). "In-vitro characterization of 3D printed PLA scaffold with hydroxyapatite-chitosan coating for mandibula reconstruction." In *AIP Conference Proceedings* (Vol. 2314, No. 1, p. 050010). AIP Publishing LLC.
[32] Arun, Y., Ghosh, R., & Domb, A. J. (2021). "Biodegradable hydrophobic injectable polymers for drug delivery and regenerative medicine". *Advanced Functional Materials*, *31*(44), 2010284.
[33] Kang, B., Hyeon, J., & So, H. (2020). "Facile microfabrication of 3-dimensional (3D) hydrophobic polymer surfaces using 3D printing technology". *Applied Surface Science*, *499*, 143733.
[34] Meng, J., Lau, C. H., Xue, Y., Zhang, R., Cao, B., & Li, P. (2020). "Compatibilizing hydrophilic and hydrophobic polymers via spray coating for desalination." *Journal of materials chemistry A*, *8*(17), 8462-8468.
[35] Li, Y., Chen, S., Wu, M., & Sun, J. (2014). "All spraying processes for the fabrication of robust, self-healing, superhydrophobic coatings". *Advanced Materials*, *26*(20), 3344-3348.
[36] Sam, E. K., Sam, D. K., Lv, X., Liu, B., Xiao, X., Gong, S., ... & Liu, J. (2019). "Recent development in the fabrication of self-healing superhydrophobic surfaces." *Chemical Engineering Journal*, *373*, 531-546.
[37] Dimitrakellis, P., & Gogolides, E. (2018). "Hydrophobic and superhydrophobic surfaces fabricated using atmospheric pressure cold plasma technology: A review". *Advances in colloid and interface science*, *254*, 1-21.
[38] Mai, Hang-Nga, Dong Choon Hyun, Ju Hayng Park, Do-Yeon Kim, Sang Min Lee, and Du-Hyeong Lee. "Antibacterial drug-release polydimethylsiloxane coating for 3d-printing dental polymer: Surface alterations and antimicrobial effects." Pharmaceuticals 13, no. 10 (2020): 304.
[39] Schneider, M., Günter, C., & Taubert, A. (2018). "Co-deposition of a hydrogel/calcium phosphate hybrid layer on 3D printed poly (lactic acid) scaffolds via dip coating: Towards automated biomaterials fabrication." *Polymers*, *10*(3), 275.
[40] Marsi, N. (2020). "Preparation and Performance Test of PEFB Reinforced Box Waste Coated Superhydrophobic Coating for Shoe Sole Application." *International Journal of Integrated Engineering*, *12*(5), 210-216.
[41] Žigon, J., Karič, M., & Pavlič, M. (2020). "Surface Finishing of 3D-Printed Polymers with Selected Coatings." *Polymers*, *12*(12), 2797.
[42] Du, B., Chen, F., Luo, R., Li, H., Zhou, S., Liu, S., & Hu, J. (2019). "Superhydrophobic surfaces with pH-induced switchable wettability for oil-water separation". *ACS omega*, *4*(15), 16508-16516.